

Report on “Radiation Disaster Recovery Studies”

Course: Environmental Radiation Protection

Name: Habibur Rahman

○Regarding “Radiation Disaster Recovery Studies”

The Fukushima Daiichi nuclear disaster, triggered by the massive earthquake and tsunami that struck Japan on March 11, 2011, stands as one of the most significant nuclear accidents in recent history[1]. The earthquake caused an immediate shutdown of the reactors, but the tsunami disabled the power supply and cooling systems required to maintain the reactors in a safe state[2]. The lack of cooling led to overheating, fuel melting, and the release of radioactive substances into the environment[3]. The Fukushima disaster prompted the evacuation of tens of thousands of residents, leaving a profound impact on the affected communities.

During 5 years of Phoenix Leader Education Programs (PLEP), various rich activities including education, training and site visiting to meet the industry, the society and government had given us valuable lesson regarding the effort to overcome the effect of radiation disaster. Four important elements worked together, including Government, private company, society, and academia, to establish a better society of Fukushima post-Earthquake and radiation disaster. Comprehensive effort to protect the public from harmful effect of radiation has been conducted including decontamination in residential area and farmland. The most important effort had come from the resident of Fukushima where they educate themselves to revive their livelihood. Residents in Fukushima played a pivotal role in the recovery process by actively participating in educational initiatives aimed at equipping themselves with the necessary knowledge to rebuild their lives[4]. This involved learning about the latest advancements in agriculture, technology, and health practices to minimize the impact of radiation on their livelihoods. Moreover, the community engaged in collaborative efforts to decontaminate residential areas and farmlands, implementing stringent measures to ensure the safety of the environment[2].

The release of radioactive substances into the environment poses a persistent and long-term risk to human health stemming from the accident[5]. The long-term consequences of the radioactive release underscore the importance of comprehensive measures to address and minimize the impact on human well-being. This underscores the urgency for ongoing monitoring, research, and strategic interventions to safeguard communities from the protracted health risks associated with the incident. In decontamination effort, the most common method used was soil removal and replacement, where contaminated soil is excavated and replaced with clean soil[6]. Another approach includes soil washing, which utilizes chemical solutions to extract and remove radioactive particles from the soil[7]. Additionally, phytoremediation employs specific plant species that can absorb and accumulate radioactive elements, facilitating the extraction of contaminants from the soil[6]. Despite these methods, radioactive decontamination encounters limitations that pose challenges to their implementation. The extent of decontamination may be constrained by the depth and spread of radioactive substances in the affected area, making complete removal difficult. Another limitation is that most of those methods would result in large amount of radioactive waste that need to be stored, both liquid and solid waste[8].

IAEA has reported lab. scale project for mixed method treatment of liquid nuclear waste in TECDOC-1336[8], including use of photocatalysis to decompose organic pollutant resulted from secondary waste. This method shows promising result in processing secondary waste problem. Advanced oxidation process (AOP) is one of promising methods because it decomposes harmful organic contaminants into harmless substances[9]. It generates hydroxyl radicals ($\bullet\text{OH}$) as a powerful reactant that can quickly destroy organic structures [10]. The advantages are no sludge generation and easy operation control [9, 11–13]. The main disadvantage of AOP is high operation cost, and in some methods, it has a slow reaction rate, making it not feasible for full-scale application [11]. One of the promising AOPs is photocatalysis, where TiO_2 was first used [14]. Visible-light photocatalysis is desirable since it is readily available by the sun, covering 46% of the sunlight [15, 16]. Later, various metal oxides were explored and developed as catalysts [17]. Hematite ($\alpha\text{-Fe}_2\text{O}_3$) has been used as a photocatalyst with the main advantages such as low cost, non-toxic, high stability, visible light absorbance, and narrow band gap [18–21]. Furthermore, the presence of H_2O_2 in hematite photocatalysis would increase the reaction drastically due to the Photo-Fenton reaction of hematite where Fe(II) resulting from photo reduction of Fe(III) then reacts with H_2O_2 to produce $\bullet\text{OH}$ [22, 23].

Magnetic separation of radioactive materials is a potential method for liquid waste treatment by modifying surface of magnetic nanoparticle[24]. By introducing specialized surface modifications to magnetic nanoparticles, the magnetic separation of radioactive materials emerges as a promising technique for liquid waste treatment and radioactive detection[24, 25]. The most important challenge regarding these applications is stability of magnetic material, where for most of liquid waste pH must be adjusted. In this regard, enhancement in stability of magnetic material is important in order to increase the effectiveness of magnetic method.

References

1. International Atomic Energy Agency. (2015) The Fukushima Daiichi Accident. International Atomic Energy Agency
2. Nea (2016) Five Years after the Fukushima Daiichi Accident NEA Nuclear Safety Improvements and Lessons Learnt
3. Baba M Fukushima accident: What happened? <https://doi.org/10.1016/j.radmeas.2013.01.013>
4. Yamashita S, Takamura N (2015) Post-crisis efforts towards recovery and resilience after the Fukushima Daiichi Nuclear Power Plant accident. *Jpn J Clin Oncol* 45:700–707
5. Dubreuil GH, Baudé S, Heriard-Dubreuil G, et al (2016) Local populations facing long-term consequences of nuclear accidents: Lessons learnt from Chernobyl and Fukushima. <https://doi.org/10.1051/radiopro/2016055>
6. Sakai M, Gomi T, Nunokawa M, et al Soil removal as a decontamination practice and radiocesium accumulation in tadpoles in rice paddies at Fukushima. <https://doi.org/10.1016/j.envpol.2014.01.002>
7. Yanaga M, Oishi A (2015) Decontamination of radioactive cesium in soil. *J Radioanal Nucl Chem* 303:1301–1304. <https://doi.org/10.1007/s10967-014-3541-z>
8. International Atomic Energy Agency. (2003) Combined methods for liquid radioactive waste treatment : final report of a co-ordinated research project 1997-2001. International Atomic Energy Agency
9. Khan JA, Sayed M, Khan S, et al (2020) Advanced oxidation processes for the treatment of contaminants of emerging concern. *Contaminants of Emerging Concern in Water and Wastewater: Advanced Treatment Processes* 299–365. <https://doi.org/10.1016/B978-0-12-813561-7.00009-2>
10. Machulek A, H. F, Gozzi F, et al (2012) Fundamental Mechanistic Studies of the Photo-Fenton Reaction for the Degradation of Organic Pollutants. *Organic Pollutants Ten Years After the Stockholm Convention - Environmental and Analytical Update*. <https://doi.org/10.5772/30995>
11. Brienza M, Katsoyiannis IA (2017) Sulfate Radical Technologies as Tertiary Treatment for the Removal of Emerging Contaminants from Wastewater. *Sustainability* 2017, Vol 9, Page 1604 9:1604. <https://doi.org/10.3390/SU9091604>
12. Priyadarshini M, Das I, Ghangrekar MM, Blaney L (2022) Advanced oxidation processes: Performance, advantages, and scale-up of emerging technologies. *J Environ Manage* 316:115295.

<https://doi.org/10.1016/J.JENVMAN.2022.115295>

13. Oyama T, Otsu T, Hidano Y, et al (2014) Remediation of aquatic environments contaminated with hydrophilic and lipophilic pharmaceuticals by TiO₂-photoassisted ozonation. *J Environ Chem Eng* 2:84–89. <https://doi.org/10.1016/j.jece.2013.11.008>
14. Hashimoto Kazuhito, Irie Hiroshi, Fujishima Akira (2005) Invited Review Paper TiO₂ Photocatalysis: A Historical Overview and Future Prospects. *Jpn J Appl Phys* 44:8269–8285
15. Zhang S, Li J, Niu H, et al (2013) Visible-light photocatalytic degradation of methylene blue using SnO₂/α-Fe₂O₃ hierarchical nanoheterostructures. *Chempluschem* 78:192–199. <https://doi.org/10.1002/cplu.201200272>
16. Li P, Terrett JA, Zbieg JR (2020) Visible-Light Photocatalysis as an Enabling Technology for Drug Discovery: A Paradigm Shift for Chemical Reactivity. *ACS Med Chem Lett* 11:2120–2130. <https://doi.org/10.1021/acsmchemlett.0c00436>
17. Satheesh R, Vignesh K, Suganthi A, Rajarajan M (2014) Visible light responsive photocatalytic applications of transition metal (M = Cu, Ni and Co) doped α-Fe₂O₃ nanoparticles. *J Environ Chem Eng* 2:1956–1968. <https://doi.org/10.1016/J.JECE.2014.08.016>
18. Gu J, Li S, Wang E, et al (2009) Single-crystalline α-Fe₂O₃ with hierarchical structures: Controllable synthesis, formation mechanism and photocatalytic properties. *J Solid State Chem* 182:1265–1272. <https://doi.org/10.1016/j.jssc.2009.01.041>
19. Li L, Chu Y, Liu Y, Dong L (2007) Template-Free Synthesis and Photocatalytic Properties of Novel Fe₂O₃ Hollow Spheres. *Journal of Physical Chemistry C* 111:2123–2127
20. Grätzel M (2001) Photoelectrochemical Cells. *Nature* 414:338–344
21. Yu J, Yu X, Huang B, et al (2009) Hydrothermal synthesis and visible-light photocatalytic activity of novel cage-like ferric oxide hollow spheres. *Cryst Growth Des* 9:1474–1480. <https://doi.org/10.1021/cg800941d>
22. Huston PL, Pignatello JJ (1999) Degradation of selected pesticide active ingredients and commercial formulations in water by the photo-assisted Fenton reaction. *Water Res* 33:1238–1246. [https://doi.org/10.1016/S0043-1354\(98\)00330-3](https://doi.org/10.1016/S0043-1354(98)00330-3)
23. Liu J, Wang B, Li Z, et al (2019) Photo-Fenton reaction and H₂O₂ enhanced photocatalytic activity of α-Fe₂O₃ nanoparticles obtained by a simple decomposition route. *J Alloys Compd* 771:398–405. <https://doi.org/10.1016/j.jallcom.2018.08.305>
24. Kaur M, Zhang H, Martin L, et al (2013) Conjugates of magnetic nanoparticle - Actinide specific chelator for radioactive waste separation. *Environ Sci Technol* 47:11942–11959. <https://doi.org/10.1021/es402205q>
25. Nugroho BS, Wijayanto H, Khoiru Wihadi MN, Nakashima S (2023) Detection of strontium species and Sr(OH)₂ NPs formation via double oxidation effect on coal oxide: Preparation and characterization of new coal oxide and its mixture. *Inorg Chem Commun* 157. <https://doi.org/10.1016/j.inoche.2023.111377>

○Title of Doctoral Thesis

⁵⁷Fe Mössbauer Studies of Ta/Nb-doped Fe₂O₃ and Application to Photocatalyst

○Summary of Doctoral Thesis

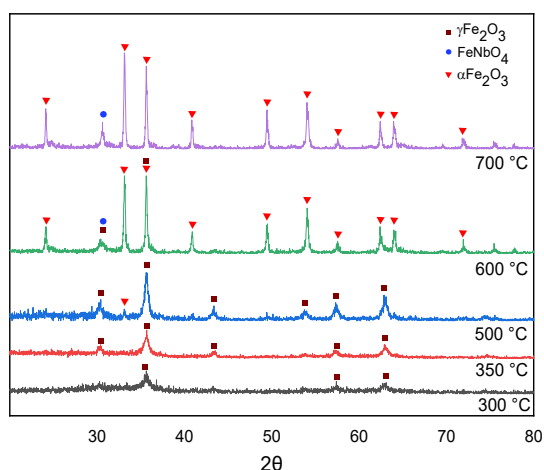


Figure 1. PXRD patterns of 9.1Nb sample.

Liquid nuclear waste remains as major problem in the industry. Recycling process frequently resulted in a large volume of secondary waste. γ -Fe₂O₃ and α -Fe₂O₃ have drawn attention for their wide range of application including magnetic separation and photo catalysis for liquid nuclear waste. The nature of γ -Fe₂O₃ is the easy transformation to α -Fe₂O₃, while α -Fe₂O₃ has low conductivity and slow catalytic activity. Several methods were used to overcome these drawbacks, one of the modifications is by doping with the other metal. Nb and Ta are group 5 elements with valence state of 5+, which have interesting characteristic such as high stability and corrosion

resistance. In the present PhD Thesis, the research focused on characterization of Nb and Ta-doped Fe_2O_3 nanoparticle and its application to the photocatalyst. General introduction is shown in Chapter 1.

In Chapter 2, niobium-doped Fe_2O_3 samples were prepared by epoxide sol-gel method at room temperature. Nb amount was changed (0, 1.9, 3.8, 5.7, 7.4 and 9.1 a.t. %). The samples were calcined at various temperatures. Sample characterization was carried out using PXRD, TEM EDS, and Mössbauer spectroscopy. Figure 1 shows PXRD patterns of 9.1Nb sample. Pure $\gamma\text{-Fe}_2\text{O}_3$ formed at 300 °C transforms completely to $\alpha\text{-Fe}_2\text{O}_3$ at 500 °C, whereas 9.1Nb sample transformed to $\alpha\text{-Fe}_2\text{O}_3$ at 600 °C. PXRD patterns show there is no other phase other than Fe_2O_3 up to 600 °C, and at 700 °C new diffraction (FeNbO_4) was observed. It was shown that the Nb doping to Fe_2O_3 suppressed the transformation of $\gamma\text{-Fe}_2\text{O}_3$ to $\alpha\text{-Fe}_2\text{O}_3$. Scherrer's equation revealed 13.0 nm of particle size

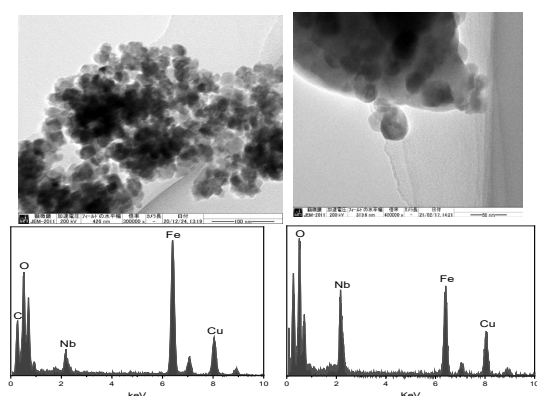


Figure 2. TEM-EDS of 9.1Nb samples calcined at 500 °C (left) and 700 °C (right).

for the sample calcined at 500 °C, 31.6 nm for 600 °C, and 35.0 nm for 700 °C. TEM EDS measurement showed particle size of 14 nm for 9.1Nb500 sample with spherical shape as shown in Figure 2. EDS confirmed that Nb is present in the Fe_2O_3 lattice. The particle became bigger by calcination at 700 °C, and new small particle appeared. EDS, PXRD, and Mössbauer revealed that the small particle is FeNbO_4 .

In Chapter 3, Mössbauer spectroscopic study on Nb-doped $\alpha\text{-Fe}_2\text{O}_3$ was conducted. For the previous report on Nb-doped $\alpha\text{-Fe}_2\text{O}_3$ [1], Fe^{3+} changed to Fe^{2+} to compensate the charge giving $\text{Nb}^{5+}\text{-}2\text{Fe}^{2+}$. Mössbauer spectra for all Nb-doped samples

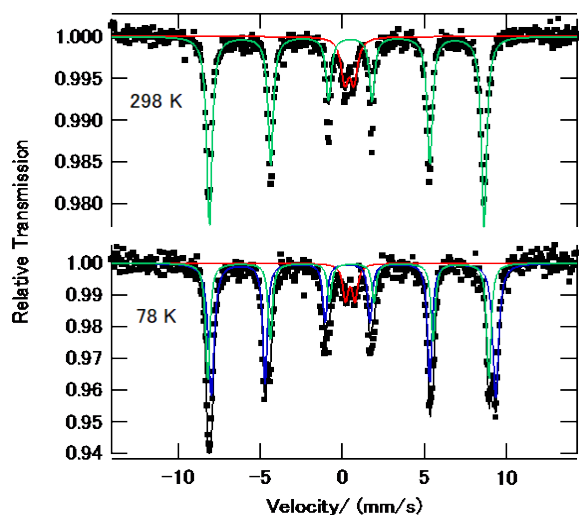


Figure 3. ^{57}Fe Mössbauer spectra at 298 and 78 K of 9.1Nb- Fe_2O_3 calcined at 700 °C

in the present study did not show Fe^{2+} state. Instead, it was suggested that small amount of Fe^{3+} was expelled from the system to compensate Nb^{5+} charge. Pure $\alpha\text{-Fe}_2\text{O}_3$ shows Morin transition (T_M) by the change of weak-ferromagnetism (WF) to anti-ferromagnetism (AF) at around 260 K which shows negative ΔE_q value for WF, while positive ΔE_q for AF in the Mössbauer spectrum. The 9.1Nb-doped $\alpha\text{-Fe}_2\text{O}_3$ calcined at 600 °C did not show T_M and it attracted to magnet. This is maybe due to ferrimagnetic-like interaction due to the existence of Nb^{5+} in the iron position. The Mössbauer parameters for the samples calcined at 700 °C showed that the weak-ferromagnetism partially exists even at lower temperature (78 K) by introducing Nb atom. One is AF iron, the other is WF iron (Fig. 3). It is thought that the Nb doping stabilizes the weak ferromagnetism even at low temperature. Figure 4 shows the area ratio of AF and WF depending on the amount of Nb. The higher the Nb doping the lower T_M . 7.4Nb700 sample shows T_M at 78K and does not attach to magnet as is typical hematite.

In Chapter 4, catalytic activity of the Nb-doped Fe_2O_3 was investigated. UV-Vis absorption spectra of $\alpha\text{-Fe}_2\text{O}_3$ sample were measured. They show strong absorption at visible light region for both pure and Nb-doped $\alpha\text{-Fe}_2\text{O}_3$. By using Tauc plot, band gap energy was calculated, and it varied from 2.13 eV for 5.7Nb700 to 2.97 eV for 5.7Nb600. Catalytic properties were measured for degradation of Methylene Blue (MB) in the presence of H_2O_2 under visible light. Figure 5 shows that the rate of degradation of MB increases with an increase of doped Nb. This shows promising catalytic activity for environmental application.

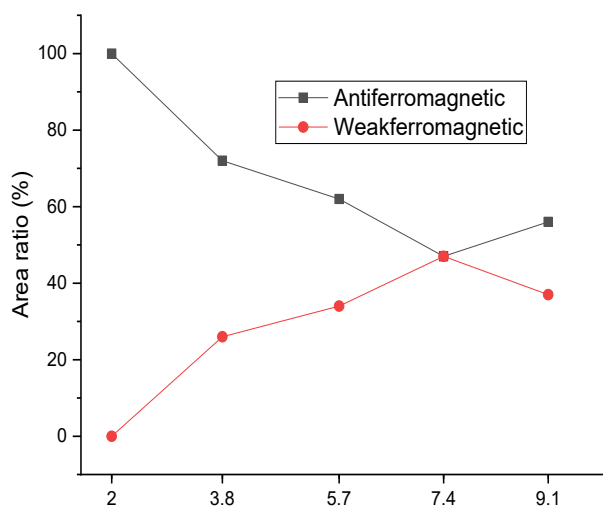


Figure 4. Area ratio of AF and WF for Nb-doped

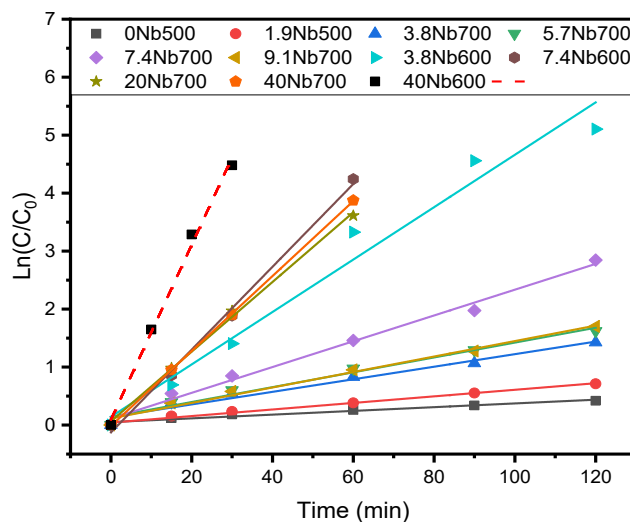


Figure 5. Photo-Fenton degradation of MB under visible

Chapter 5 is the study for Ta-doped Fe_2O_3 . Ta doping showed that the stability of $\gamma\text{-Fe}_2\text{O}_3$ increased and the magnetic properties of hematite changed. For the 7.4Ta700 sample, the particle shows large size of 300nm but there is no T_M at 78K. Ionic radii of Ta^{5+} and Nb^{5+} are the same with 0.64\AA , but the lattice constant of Ta is reported to be longer than Nb, which makes Ta have more influence to the lattice arrangement of hematite.

Chapter 6 shows general conclusions. Introduction of Nb and Ta to Fe_2O_3 suppresses the phase transformation from maghemite to hematite. Nb and Ta are incorporated to $\gamma\text{-Fe}_2\text{O}_3$ lattice by filling vacancy and replacing Fe position, stabilizing $\gamma\text{-Fe}_2\text{O}_3$. Nb/Ta atoms were expelled from lattice during transformation to $\alpha\text{-Fe}_2\text{O}_3$. Nb/Ta also greatly affect the magnetic properties by lowering the Morin Transition temperature (T_M). The catalytic activity of sample is increased by the increase of Nb doping.

Reference

- [1] Sanchez C et al., J Solid State Chem 61:47–55 (1986).

Other theses published in academic research journals

- ^{57}Fe Mössbauer spectroscopic study on the magnetic structure of niobium-doped hematite

H. Rahman, S. Nakashima

Applied Physics A, DOI: 10.1007/s00339-022-05691-x

- Stabilization of $\gamma\text{-Fe}_2\text{O}_3$ Nanoparticles to Heat by Doping Nb and Its Property Studied by Mössbauer Spectroscopy

H. Rahman, S. Nakashima

Submitted to Journal of Magnetism and Magnetic Materials (under revision)

3. Catalytic Activity of Ferrimagnet-Like Nb-Doped α -Fe₂O₃ with Heterojunction Structure

Habibur Rahman, Bofan Zhang, Shiro Kubuki, Satoru Nakashima

Submitted to Inorganic Chemistry Communications

4. ⁵⁷Fe Mössbauer Spectroscopic Study on the Magnetic Properties of Tantalum-Doped Maghemite and Hematite

H. Rahman, S. Nakashima

Accepted at Hyperfine Interactions